Development of a Neutron Radiography System based on a 10 MeV Electron Linac

Jacob G. Fantidis[1*], G. E. Nicolaou[2]
1- Department of Electrical Engineering-Department of Physics, International Hellenic University, Agios Loukas, 65404 Kavala, Greece.
Email: fantidis@teiemt.gr (Corresponding author)
2- Laboratory of Nuclear Technology, Department of Electrical and Computer Engineering, 'Democritus' University of Thrace, Xanthi, Greece.
Email: nicolaou@ee.duth.gr

Received: March 2020 Revised: May 2020 Accepted: July 2020

ABSTRACT:
A thermal neutron radiography unit using the neutrons which emits a 10 MeV electron linac compact has been designed and simulated via MCNPX Monte Carlo code. The facility was carried out for an extensive range of values for the collimator ratio L/D, the main parameter which describes the quality of the produced radiographic images. The results show that the presented facility provides high thermal neutron flux; while with the use of single sapphire filter fulfills all the suggested values which characterize a high quality thermal neutron radiography system. A comparison with other similar facilities indicates that the use of a photoneutron source using a 10 MeV electrons beam is a useful substitutional for radiographic purposes.

KEYWORDS: Neutron Radiography, MCNPX, Electron Medical Linac, Fast Neutron Filter.

1. INTRODUCTION

Penetrating radiation has been used for imaging purposes from 1895 when Roentgen discovered X-rays. Neutron Radiography (NR) represents the most common method of Non-Destructive Testing (NDT) because NR is a useful imaging technique in order to evaluate the internal structure of the materials. Neutron interacts with materials in a complementary way compared to the X-ray imaging. X-rays interact with the electron clouds of atoms, and have cross sections which are analogous to their atomic number. Conversely neutrons interrelate with atomic nuclei. Note that there is not dependence between atomic number and the respectively cross sections; compared to x- and γ- rays, neutrons can be attenuated by many light materials, i.e. hydrogen or carbon, however can penetrate many heavy materials. This implies that NR can yield information in cases where X-ray radiography fails.

Thermal neutrons are usually used for NR imaging because most materials show higher attenuation for low energy neutrons. For this reason, thermal NR is the most popular NR NDT method used in many fields of research and industry such as security applications [1]-[9] medicine [10-17], material sciences [18-29], geology [30], archeology [31-32] etc. A suitable neutron beam is necessary in order to establish a thermal NR facility. Today the numbers of thermal NR facilities remain limited owing to the fact that these facilities are based mainly in nuclear research reactors [33]. In order to overcome the lack of the nuclear reactors, the required neutron beams usually are derived by accelerators or from some isotopic sources. A typical facility includes Deuterium-Tritium (DT) [34], Deuterium-Deuterium (DD) [34]-[37], Tritium-Tritium (TT) [34], [38] neutron generators, ^{252}Cf [39-41], ^{241}Am/Be [42-44] isotopic neutron sources, proton [45] or electron [46] usually on accelerators on beryllium [10], [47-50] or lithium [51] targets.

A high quality thermal NR facility must satisfy some recommended values (Table 1). The primary goal of the presented work is to propose a thermal NR facility using as neutron source, a medical electron linear accelerator (Linac), which produces electron with 10 MeV energy and fulfills all the suggested values in order to produce quality radiographic images [52]. The unit has been planned and simulated via the MCNPX 2.5.0 code for an extensive range of the relevant factors [53]. Comparisons of the proposed unit with other similar thermal facilities which use neuron beams from nonnuclear reactor sources are also presented.

Paper type: Research paper
DOI: https://doi.org/10.29252/mjee.14.4.21
How to cite this paper: J. G. Fantidis, G. E. Nicolaou, **"Development of a Neutron Radiography System based on a 10 MeV Electron Linac"**, *Majlesi Journal of Electrical Engineering*, Vol.14, No. 4, pp. 21-28, 2020.

Table 1. Suggested values for different neutron beam parameters with the aim of high quality radiographic images.

f_{th} ($ncm^{-2}s^{-1}$)	L/D ratio	TNC (%)	n/γ ratio ($n\ cm^{-2}\ mSv^{-1}$)
$\geq 10^6$	≥ 90	≥ 90	$\geq 10^4$

2. MATERIALS AND METHODS

2.1. Neutron Source

According to the previous works, owing to the high atomic number and its physicochemical characteristics, tungsten is one of the best materials as electron target for (e, γ) reaction [54-58]. For (γ, n) reaction a cylindrical D_2O target was considered. The geometrical configuration which is presented here is based on previous work from Tatari and Ranjbar with modifications in order to adapt the photoneutron source which firstly was designed for radiotherapy purposes as photoneutron source for thermal NR units. A 10 MeV electron linac that has been considered in this work has the parameters which are listed in Table 2 [59].

Table 2. The LINAC beam parameters based on previous work from Tatari and Ranjbar [59].

Parameter	Value
Energy	10 MeV
Current	50 mA
Pulse repetition rate	300 Hz
Pulse duration	3.6 μs
Average beam power	540 W

The geometrical configuration of the source is shown in Fig. 1. The primary goal of the source is to maximize the thermal neutron flux at the exit window. The tungsten target is a disk with radius 1.5 cm and 0.15 cm thickness. The (γ, n) convertor is a rectangular filled with D_2O with dimensions of 64x64x9 cm. Beryllium reflectors with 50 cm depth surround the neutron source and increase the neutron flux with a conical head design at the exit aperture of the source. High Density Polyethylene (HD-PE) is the best moderator material [39, 60] and according to our simulations, 1.8 cm provides the maximum thermal neutron flux (f_{th}) (Fig. 2) at the exit of the beam while with the intention to filter the undesired epithermal and fast neutrons, a conical single sapphire filter can be installed before the exit aperture. The single sapphire is maybe the best material for the filtering of the fast neutrons [61]. Fig. 3 depicts the neutron spectrum at the exit aperture.

2.2. Thermal Neutron Collimator

The parameter which affects mainly the quality of a thermal NR unit is the collimator ratio *L/D* [62] and described by the equations:

$$\phi_i = \frac{\phi_\alpha}{16}\left(\frac{D}{L_S}\right)^2 \quad (1)$$

and

$$u_g = L_f \frac{D}{L_s} \quad (2)$$

Where, φ_i expresses the neutron flux at the image position, φ_a denotes the neutron flux at the aperture position, L_s is the distance between the neutron source and the investigated sample, D indicates the diameter of the inlet aperture, u_g specifies the geometric unsharpness and L_f expresses the distance between the image and the investigated object (equal to 0.5 cm).

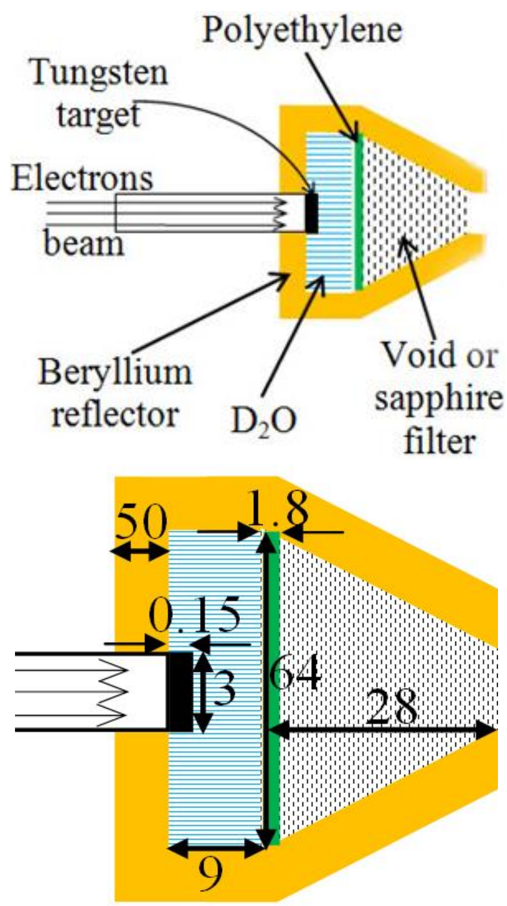

Fig. 1. Geometrical configuration of the photoneutron source (up) and its dimensions (down all dimensions in cm).

In addition, the effectiveness of the neutron beam is described by the beam divergence which is expressed by the formula [63]-[65]

$$\theta = \tan^{-1}\left(\frac{I}{2L}\right) \quad (3)$$

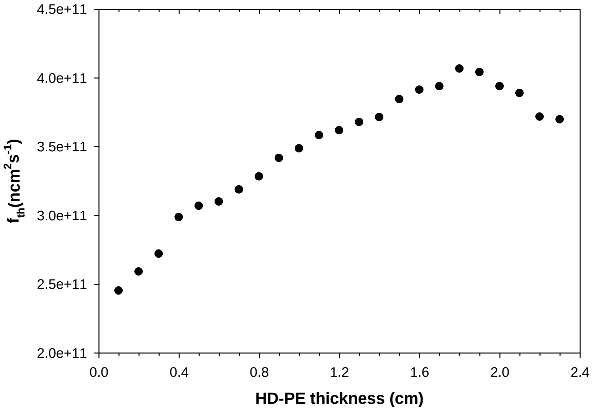

Fig. 2. The Thermal neutron flux at the exit of the source configuration, for different thicknesses of the high density polyethylene moderator.

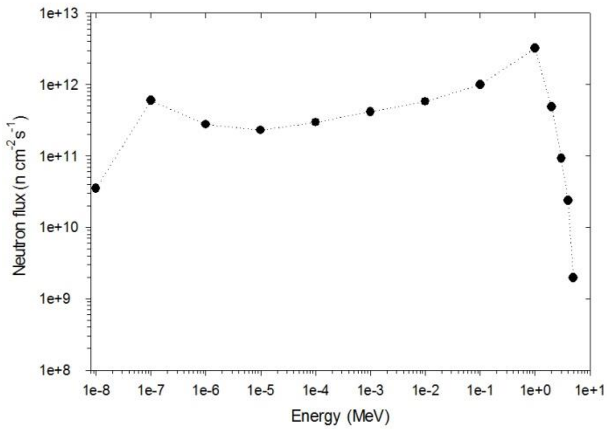

Fig. 3. The neutron spectrum at the exit aperture.

Where, θ denotes the half-angle of the beam divergence, I indicates the bigger dimension of the radiographic image while L defines the collimator length. Last but not least, two others important parameters are the TNC (the ratio of thermal neutron flux to total neutron flux) and the n/γ ratio which defines the neutron intensity versus the gamma components in the beam. In accordance with Hawkesworth, the n/γ ratio should be higher than 10^4 $ncm^{-2}mSv^{-1}$ that minimum recommended value is 500 $ncm^{-2}mSv^{-1}$ [66].

The geometrical configuration was designed and simulated in this article is presented in Fig. 4. Next to the aperture of the neutron source, there is a diverging collimator which has variable length (L = 200-800 cm). The material of the collimator is a very important part of the unit and must stop scattered neutrons to reach at the investigated object position. A previous work from Fantidis [44] has shown that boral offers better performance than cadmium or gadolinium. The filling materials must stop both neutrons and gamma so a combination of borated polyethylene (PE-B) and bismuth is a good choice. Lead has better performance than bismuth but is a hazardous material so the bismuth is a safer choice. Boral with 0.8 cm -thickness was selected as lining material while borated polyethylene (PE-B) was chosen as a filling material with 3.8 thickness and bismuth (Bi) with 1.2 cm depth was chosen like the collimator casing. The aperture size of the collimator (D) was 4 cm and designed as a combination of 2 materials, i) a 0.8 cm layer of boral with the purpose to minimize stray and scattered neutrons from the inspected object and ii) from 1.2 cm of Bi with the goal to absorb the unwanted γ-rays. All these dimensions are the minimum in order to the presented facility to meet the criterion $n/\gamma \geq 10^4$ n cm^{-2} mSv^{-1} and were derived after numerous simulations. The aperture in the side of the image position (D_0) was selected equal to 12 cm.

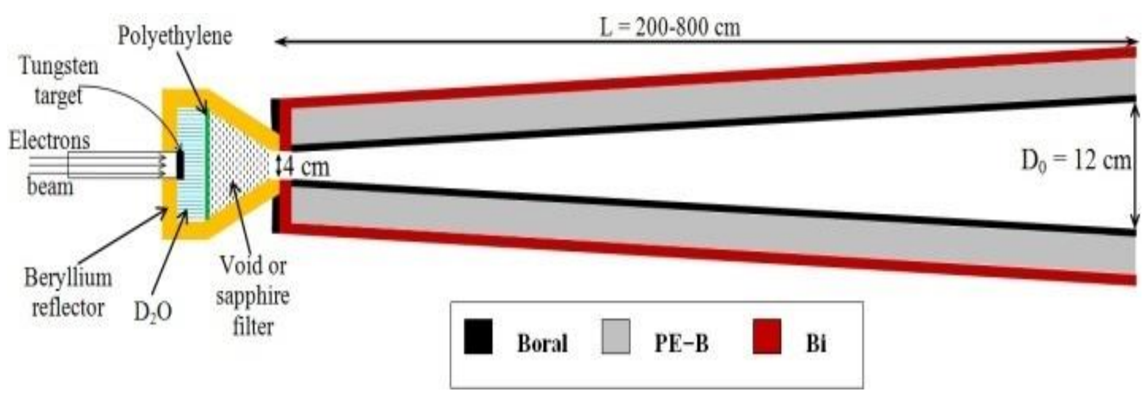

Fig. 4. Geometric configuration of the studied facility.

3. RESULTS AND DISCUSSION

For the configuration presented in Fig. 4, the basic simulated parameters of the system namely, the thermal neutron flux (f_{th}), the TNC ratio and the n/γ ratio are shown in Table 3 for five values of the L/D ratio (50, 75, 100, 150 and 200). The divergence angle (θ) of the beam has a range between θ = 0.43 – 1.71° while the U_g varies from 2.5×10^{-3} up to 10^{-2}. The f_{th} (with energy 0.01–0.3 eV) has values from 6.11×10^5 up to 1.01×10^7 $ncm^{-2}s^{-1}$, the TNC is approximately the same (with values 3.35-3.39%) while the n/γ ratio is above of the recommended value in each case. According to the suggested values (Table 1) the main problem is the poor results for the TNC ratio.

With the intention to overcome the low values of the TNC, the present of the single sapphire as fast/epithermal neutron filter is required [49]. Table 4 shows the f_{th}, the TNC ratio and the n/γ ratio for three different L/D values (50, 100 and 150) and for five different depths (5, 10, 15, 20 and 25 cm) of single sapphire filter. From the results presented, it concluded that the TNC ratio is practically constant for the equal thickness of the sapphire filter and practical independent of the L/D ratio. 5 cm of single sapphire reduces the f_{th} approximately 18% while the TNC is about 11-12%. At the same time the n/γ ratio decreases more than 40%, however remains above the recommended values. 10 and 15 cm thicknesses of sapphire filter provide TNC around of 34% and 67% respectively while the f_{th} has lower values than the case without sapphire filter by more than 31% and 41% correspondingly. The use of 20 cm single sapphire as fast neutron filters although can reduce more than a half the f_{th} provides TNC values close to the desired value. With 25 cm sapphire filter, the facility satisfies all the suggested values hence the presented unit is capable to provide quality thermal radiographies.

Fig. 5 shows the neutron spectra in a plane 0.5 cm away from the outlet of the converging collimator for 6 different occasions, without neutron filter and with 5, 10, 15 20 and 25 cm sapphire filter. It is evident that the presence of the filter reduces drastically the presence of the fast neutrons in the beam while the f_{th} does not have analogous decrement. In order to evaluate the presented facility, a comparison with other thermal NR units which do not use nuclear reactor as neutron sources was done (Table 5). The proposed facility offers a far better performance than isotopic neutron sources and neutron generators. Moreover this unit surpasses many other which is based on proton accelerators. These results indicate that the presented thermal NR unit which is based on a 10 MeV electron linac is an interesting option for quality thermal neutron imaging.

Table 3. Thermal NR simulated factors for a range of L/D ratio values.

L (cm)	L/D	θ (deg)	U_g (cm)	f_{th} ($ncm^{-2}s^{-1}$)	n/γ ($cm^{-2}mSv^{-1}$)	TNC (%)
200	50	1.71	1.00E-2	1.01E+07	3.05E+04	3.35
300	75	1.14	6.67E-3	4.39E+06	2.81E+04	3.33
400	100	0.86	5.00E-3	2.47E+06	2.68E+04	3.36
500	125	0.69	4.00E-3	1.55E+06	2.34E+04	3.35
600	150	0.57	3.33E-3	1.08E+06	2.29E+04	3.35
800	200	0.43	2.50E-3	6.11E+05	2.25E+04	3.39

Table 4. Simulated parameters for 3 L/D ratio values and 5 different depths of fast neutron filter.

	L/D = 50			L/D = 100			L/D = 150		
Sapphire filter	f_{th} ($ncm^{-2}s^{-1}$)	n/γ ($cm^{-2}mSv^{-1}$)	TNC (%)	f_{th} ($ncm^{-2}s^{-1}$)	n/γ ($cm^{-2}mSv^{-1}$)	TNC (%)	f_{th} ($ncm^{-2}s^{-1}$)	n/γ ($cm^{-2}mSv^{-1}$)	TNC (%)
0	1.01E+07	3.05E+04	3.35	2.47E+06	2.68E+04	3.36	1.08E+06	2.29E+04	3.35
5	8.23E+06	1.57E+04	11.65	2.04E+06	1.37E+04	11.59	8.86E+05	1.34E+04	12.06
10	6.94E+06	1.83E+04	33.41	1.72E+06	1.02E+04	34.75	7.47E+05	1.01E+04	35.21
15	5.84E+06	1.04E+04	64.88	1.45E+06	1.02E+04	67.18	6.29E+05	1.02E+04	67.62
20	4.94E+06	1.03E+04	86.75	1.22E+06	1.04E+04	88.31	5.32E+05	1.08E+04	88.47
25	4.36E+06	1.24E+04	95.99	1.08E+06	1.50E+04	96.42	4.79E+05	1.05E+04	96.58

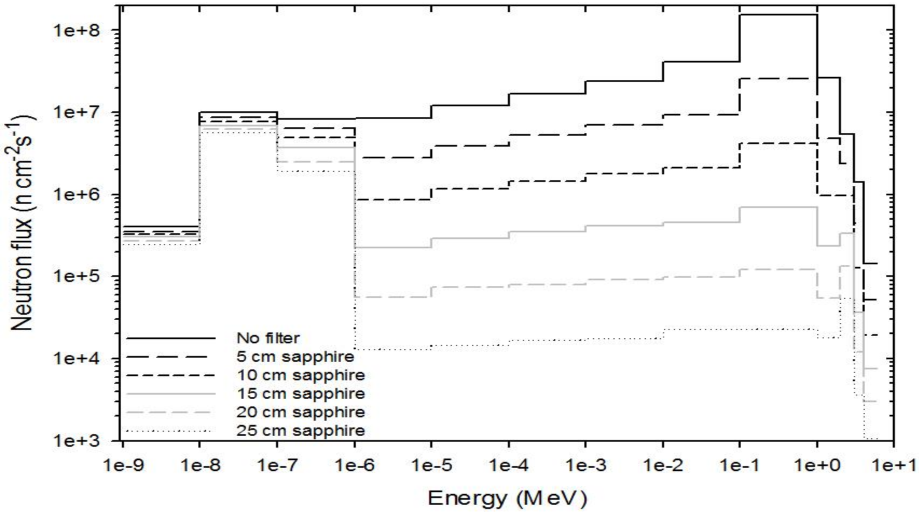

Fig. 5. Neutron spectra in a plane 0.5 cm away from the output of the collimator for 6 different simulations.

Table 5. Comparison of the presented unit with other previous published works.

Source	Total Neutron yield (ns^{-1})	$f_{thermal}$ (n cm^{-2}s^{-1})	TNC (%)	n/γ (cm^{-2}mSv^{-1})	L/D
10MeV 50 mA electron Linac	6.25×10^{12}	1.01×10^{7} 4.36×10^{6} 2.47×10^{6} 1.08×10^{6}	3.35 95.99 3.36 96.42	3.05×10^{4} 1.25×10^{4} 2.68×10^{4} 1.50×10^{4}	50 50 100 100
25MeV 1 mA electron Linac [40]	5.78×10^{13}	2.23×10^{7} 1.60×10^{7} 2.70×10^{6}	16.27 68.06 92.31	$>10^{7}$	50 50 50
^{252}Cf radioisotope 50mg [39]	1.157×10^{11}	3.703×10^{4}			50
^{252}Cf radioisotope 50mg [40]	1.157×10^{11}	1.57×10^{4} 6.28×10^{3} 4.18×10^{3} 2.76×10^{3}	0.51 30.06 0.15 1.97	9.71×10^{3} 1.41×10^{4} 9.92×10^{3} 1.53×10^{4}	50 50 100 100
^{252}Cf radioisotope 50mg [41]	1.157×10^{11}	2.85×10^{4} 1.90×10^{4} 7.72×10^{3} 5.16×10^{3}	3.48 13.83 1.09 4.54	4.50×10^{4} 2.69×10^{4} 6.53×10^{4} 2.89×10^{4}	50 50 100 100
^{241}Am/Be radioisotope 1000Ci [38]	2.7×10^{9}	6.102×10^{2} 3.537×10^{2}	5.41 22.12	$>10^{6}$	50 50
DD neutron generator [35]	10^{11}	1.58×10^{4} 9.66×10^{3} 4.12×10^{3} 2.52×10^{3}	3.57 27.06 3.89 33.95	7.01×10^{6} 6.47×10^{4} 1.01×10^{6} 7.75×10^{4}	50 50 100 100
DD neutron generator [36]	10^{9}	2.21×10^{4} 7.69×10^{3} 1.22×10^{3}	33 49 16	2.83×10^{6} 1.02×10^{6} 1.10×10^{6}	50 50 100
DT neutron generator [34]	1×10^{13}	3.81×10^{5} 8.99×10^{4}	0.46 0.49	7.25×10^{7} 7.29×10^{7}	50 100
TT neutron generator [34]	10^{11}	8.83×10^{3} 2.36×10^{3}	2.02 2.11	4.38×10^{7} 6.44×10^{7}	50 100
2.5 MeV 10mA proton linac [51]	8.83×10^{12}	2.72×10^{6} 1.63×10^{6} 6.64×10^{5} 3.98×10^{5}	16.82 84.60 16.93 84.94	2.98×10^{8} 5.47×10^{7} 3.79×10^{8} 7.64×10^{7}	50 50 100 100

4 MeV 1mA proton linac [45]	1.2×10^{12}	4.75×10^{5} 3.10×10^{5} 1.19×10^{5} 7.79×10^{4}	12.50 74.61 12.83 75.86	$>10^{6}$	50 50 100 100
15 and 20 MeV 200μA proton linac [50]	7.87×10^{12} 1.32×10^{13}	2.22×10^{5} 3.86×10^{5}	84.9 87.2	2.39×10^{8} 2.01×10^{8}	90 90

4. CONCLUSION AND REMARKS

A facility for thermal neutron radiography purposes, which is based on a neutron beam emitted from a 10 MeV medical electron linac, has been simulated with the help of the MCNPX Monte Carlo code. A tungsten disk was selected as e-γ converter and heavy water as γ-n converter. Moreover, high density polyethylene and beryllium were selected as moderator and reflector materials respectively while for the collimator design, Boral was chosen as the lining material and borated polyethylene and bismuth as the filling materials. The addition of a single sapphire for the filtering of the fast neutrons improves drastically the percentage of the thermal neutrons in the beam. The presented unit was simulated for a wide range of the factors which characterized a thermal neutron radiography facility and the results indicate that the presented facility meets all the recommended values which are essential for high quality neutron radiographic images. Last but not least, the comparison between the simulated facility with some published units shows that the use of a medical electron linac for the production of high quality thermal neutron radiographies is possible.

REFERENCES

[1] Z. Chen, and X. Wang, **"Cargo X-ray imaging technology for material discrimination,"** *Port Technol. Int*, Vol. 30, pp. 163-165, 2006

[2] J. E. Eberhardt, Y. Liu, S. Rainey, G. J. Roach, R. J. Stevens, B. D. Sowerby, and J. R. Tickner. **"Fast neutron and gamma-ray interrogation of air cargo containers,"** In *International Workshop on Fast Neutron Detectors, Cape Town*, pp. 3-6. April 2006.

[3] A. Buffler, and J. Tickner, "Detecting contraband using neutrons: challenges and future directions," *Radiation Measurements*, Vol. 45, No. 10, 1186-1192, 2010.

[4] J. G. Fantidis, and G. E. Nicolaou, **"A transportable fast neutron and dual gamma-ray system for the detection of illicit materials,"** *Nuclear Instruments and Methods in Physics Research Section A: Accelerators, Spectrometers, Detectors and Associated Equipment*, Vol. 648, No. 1, pp. 275-284, 2011.

[5] Y. Takahashi, T. Misawa, C. H. Pyeon, S. Shiroya, and K. Yoshikawa, **"Landmine detection method combined with backscattering neutrons and capture γ-rays from hydrogen,"** *Applied Radiation and Isotopes*, Vol. 69, No. 7, pp. 1027-1032, 2011.

[6] N. Elsheikh, G.Viesti, I. ElAgib, and F. Habbani, **"On the use of a (^{252}Cf–^{3}He) assembly for landmine detection by the neutron back-scattering method,"** *Applied Radiation and Isotopes*, Vol. 70, No. 4, pp. 643-649, 2012.

[7] J. G. Fantidis, and G. E. Nicolaou, **"Multiple fast neutron and gamma-ray beam systems for the detection of illicit materials,"** *Journal of Radioanalytical and Nuclear Chemistry*, Vol. 295, No. 2, pp. 973-977. 2013

[8] J. G. Fantidis, A. Dalakas, C. Potolias, K. Karakoulidis, and P. Kogias, **"A Fast Neutron and Gamma Ray System for the Detection of Illicit Materials Based on Simple Isotopic Sources,"** *Journal of Engineering Science & Technology Review*, Vol. 9, No. 6. pp. 58-58, 2016.

[9] J. Rahon, A. Danagoulian, T. D. MacDonald, Z. S. Hartwig, and R. C. Lanza, **"Spectroscopic neutron radiography for a cargo scanning system,"** *Nuclear Instruments and Methods in Physics Research Section A: Accelerators, Spectrometers, Detectors and Associated Equipment*, Vol. 820, pp. 141-145, 2016.

[10] J. G. Fantidis, G. Nicolaou, and N. F. Tsagas, **"A Monte Carlo simulation of neutron activation analysis of bulk objects,"** *Radiation Measurements*, Vol. 44, No. 3, pp. 273-277, 2009.

[11] A. A. Naqvi, M. Maslehuddin, M. A. Garwan, M. M. Nagadi, O. S. B. Al-Amoudi, and M. Raashid, **"Effect of silica fume addition on the PGNAA measurement of chlorine in concrete,"** *Applied Radiation and Isotopes*, Vol. 68, No. 3, pp. 412-417, 2010.

[12] J. G. Fantidis, G. E. Nicolaou, C. Potolias, N. Vordos, and D. V. Bandekas, **"The comparison of four neutron sources for Prompt Gamma Neutron Activation Analysis (PGNAA) in vivo detections of boron,"** *Journal of radioanalytical and nuclear chemistry*, Vol. 290, No. 2, pp. 289-295, 2011.

[13] F. S. Rasouli and S. F. Masoudi, **"Design and optimization of a beam shaping assembly for BNCT based on D–T neutron generator and dose evaluation using a simulated head phantom,"** *Applied Radiation and Isotopes*, Vol. 70, No. 12, pp. 2755-2762, 2012.

[14] Y. Kasesaz, H. Khalafi, and F. Rahmani, **"Optimization of the beam shaping assembly in the D–D neutron generators-based BNCT using the response matrix method,"** *Applied Radiation and Isotopes*, Vol. 82, pp. 55-59, 2013.

[15] F. Torabi, S. F. Masoudi, F. Rahmani, F. S. Rasouli, **"BSA optimization and dosimetric assessment for an electron linac based BNCT of deep-seated brain tumors,"** *Journal of Radioanalytical and Nuclear Chemistry*, Vol. 300, No. 3, pp. 1167-1174. 2014.

[16] J. G. Fantidis and A. Antoniadis, **"**Optimization study for BNCT facility based on a DT neutron generator**,"** *Int. J. Radiat. Res*, Vol. 13, No. 1, pp. 13-24, 2015.

[17] J. G. Fantidis and G. Nicolaou, **"Optimization of**

Beam Shaping Assembly design for Boron Neutron Capture Therapy based on a transportable proton accelerator," *Alexandria engineering journal,* Vol. 57, No. 4, pp. 2333-2342, 2017.

[18] M. Sedighi-Gilani, M. Griffa, D. Mannes, E. Lehmann, J. Carmeliet, and D. Derome, **"Visualization and quantification of liquid water transport in softwood by means of neutron radiography,"** *International Journal of Heat and Mass Transfer*, Vol. 55, No. 21-22, pp. 6211-6221, 2012.

[19] A. El Abd, A. M. Abdel-Monem, and W. A. Kansouh, **"Experimental determination of moisture distributions in fired clay brick using a ^{252}Cf source: A neutron transmission study,"** *Applied Radiation and Isotopes*, Vol. 74, pp. 78-85, 2013.

[20] Y. Polsky, L. M. Anovitz, P. Bingham, and J. Carmichael, **"Application of neutron imaging to investigate flow through fractures for EGS,"** In *Proc. 38th workshop on geothermal reservoir engineering, Stanford Univ., Stanford, CA*, February 2013.

[21] C. Villani, C. Lucero, D. Bentz, D. Hussey, D. L. Jacobson, and W. J. Weiss, **"Neutron radiography evaluation of drying in mortars with and without shrinkage reducing admixtures,"** In *American Concrete Institute Fall Meeting, Washington, DC,* Vol. 26, October 2014.

[22] A. Griesche, E. Dabah, & T. Kannengießer, **"Neutron imaging of hydrogen in iron and steel,"** *Canadian Metallurgical Quarterly*, Vol. 54, No. 1, pp. 38-42, 2015.

[23] R. J. Shypailo, **"Stability evaluation and correction of a pulsed neutron generator prompt gamma activation analysis system,"** *Journal of Radioanalytical and Nuclear Chemistry*, Vol. 307, No. 3, pp. 1781-1786, 2016.

[24] M. K. Moradllo, S. R. Reese, and W. Jason Weiss. **"Using Neutron Radiography to Quantify the Settlement of Fresh Concrete,"** *Advances in Civil Engineering Materials,* Vol. 8.1, pp. 71-87, 2019,

[25] M. K. Moradllo, C. Qiao, H. Hall, M. T. Ley, S. R. Reese, and W. J. Weiss **"Quantifying fluid filling of the air voids in air entrained concrete using neutron radiography,"** *Cement and Concrete Composites*, Vol. 104, 103407, 2019.

[26] N. Alderete, Y. V. Zaccardi, D. Snoeck, B. Van Belleghem, P. Van den Heede, K. Van Tittelboom, and N. De Belie, **"Capillary imbibition in mortars with natural pozzolan, limestone powder and slag evaluated through neutron radiography, electrical conductivity, and gravimetric analysis,"** *Cement and Concrete Research*, Vol. 118, pp. 57-68, 2019.

[27] J. M., Campillo-Robles, D., Goonetilleke, D., Soler, N., Sharma, D. M., Rodríguez, T., Bücherl,... & V. Karahan, **"Monitoring lead-acid battery function using operando neutron radiography,"** *Journal of Power Sources,* Vol.438, 226976, 2019

[28] N. Di Luozzo, M. Schulz, and M. Fontana, **"Imaging of boron distribution in steel with neutron radiography and tomography,"** *Journal of Materials Science*, pp. 1-11, 2020.

[29] A. El Abd, S. E. Kichanov, M. Taman, and K. M. Nazarov, **"Penetration of water into cracked geopolymer mortars by means of neutron radiography,"** *Construction and Building Materials*, 119471, 2020.

[30] Joos, G. Schmitz, M. J. Mühlbauer, and B. Schillinger, **"Investigation of moisture phase change in porous media using neutron radiography and gravimetric analysis,"** *International Journal of Heat and Mass Transfer*, Vol. 53, No. 23-24, pp. 5283-5288, 2010

[31] D. S. Hussey, and D. L. Jacobson, **"Applications of neutron imaging and future possibilities,"** *Neutron News*, Vol. 26, No.2, pp. 19-22, 2015.

[32] E. Lehmann, P. Trtik, and D. Ridikas, **"Status and perspectives of neutron imaging facilities,"** *Physics Procedia*, Vol. 88, pp. 140-147, 2017.

[33] International Atomic Energy Agency Retrieved from https://nucleus.iaea.org/RRDB/RR/ReactorSearch.aspx?

[34] J. G. Fantidis, B. V. Dimitrios, P. Constantinos, and N. Vordos, **"Fast and thermal neutron radiographies based on a compact neutron generator,"** *Journal of Theoretical and Applied Physics*, Vol. 6, No. 1, 20. 2012

[35] J. G., Fantidis, G. E., Nicolaou, and N. F. Tsagas, **"Optimization study of a transportable neutron radiography unit based on a compact neutron generator,"** *Nuclear Instruments and Methods in Physics Research Section A: Accelerators, Spectrometers, Detectors and Associated Equipment*, Vol. 618, No. 1-3, pp. 331-335, 2010.

[36] K. Bergaoui, N. Reguigui, C. K. Gary, J. T. Cremer, J. H. Vainionpaa, and M. A. Piestrup, **"Design, testing and optimization of a neutron radiography system based on a Deuterium–Deuterium (D–D) neutron generator,"** *Journal of Radioanalytical and Nuclear Chemistry*, Vol. 299, No. 1, pp. 41-51, 2014.

[37] M. Taylor, E. Sengbusch, C. Seyfert, E. Moll, & R. Radel, **"Thermal neutron radiography using a high-flux compact neutron generator,"** *Physics Procedia*, Vol.88, pp. 175-183, 2017.

[38] E. Lehmann, G. Frei, A. Nordlund, & B. Dahl, **"Neutron radiography with 14 MeV neutrons from a neutron generator,"** *IEEE transactions on nuclear science*, Vol. 52, No. 1, pp. 389-393, 2005.

[39] A. X. Da Silva, and V. R. Crispim, **"Study of a neutron radiography system using ^{252}Cf neutron source,"** *Radiation Physics and Chemistry*, Vol. 61, No. 3-6, pp. 515-517, 2001.

[40] J. Fantidis, G. Nicolaou, & N. Tsagas, **"A transportable neutron radiography system,"** *Journal of radioanalytical and nuclear chemistry*, Vol. 284, No. 2, pp. 479-484. 2010.

[41] J. G., Fantidis, C., Potolias, N., Vordos, & D. V. Bandekas, **"Optimization study of a transportable neutron radiography system based on a ^{252}Cf neutron source,"** *Moldavian J Phys Sci*, Vol. 10, No. 1, pp. 121-130, 2011.

[42] U. Pujala, L. Thilagam, T. S. Selvakumaran, D. K. Mohapatra E. A. Raja, K. V. Subbaiah, and R. Baskaran, **"Analysis of neutron streaming through**

the trenches at linac based neutron generator facility," IGCAR. *Radiation Protection and Environment*, Vol. 34, No. 4, pp. 262-266, 2011.

[43] H. Jafari, & S. A. H. Feghhi, **"Design and simulation of neutron radiography system based on ^{241}Am–Be source,"** *Radiation Physics and Chemistry*, Vol. 81, No. 5, pp. 506-511, 2012.

[44] J. G. Fantidis, **"Comparison of different geometric configurations and materials for neutron radiography purposes based on a ^{241}Am/Be neutron,"** *Journal of Taibah University for Science*, Vol. 11, No. 6, pp. 1214-1220, 2017.

[45] J. G. Fantidis, D. V. Bandekas, & N. Vordos, **"The replacement of research reactors with a compact proton linac for neutron radiography,"** *Radiation Physics and Chemistry*, Vol.86, pp. 74-78, 2013.

[46] J. G. Fantidis, **"The use of electron linac for high quality thermal neutron radiography unit,"** *Nuclear Instruments and Methods in Physics Research Section A: Accelerators, Spectrometers, Detectors and Associated Equipment*, Vol. 908, pp. 361-366, 2018.

[47] T. Bücherl, N. Kardjilov, C. L. von Gostomski, E. Calzada, and A. M. ELGhobary, **"A mobile neutron source based on the SbBe reaction,"** *Applied radiation and isotopes*, Vol. 61, No. 4, pp. 659-662, 2004.

[48] T. Bucherl, N. Kardjilov, C. L. Von Gostomski, and E. Calzada, **Performance studies of a mobile neutron source based on the SbBe reaction,"** *IEEE transactions on nuclear science*, Vol.b52, No. 1, pp. 342-345, 2005.

[49] Y. Zou, W. Wen, Z. Guo, Y. Lu, S. Peng, K. Zhu and Q. Zhou, **"PKUNIFTY: A neutron imaging facility based on an RFQ accelerator,"** *Nuclear Instruments and Methods in Physics Research Section A: Accelerators, Spectrometers, Detectors and Associated Equipment*, Vol. 651, No. 1, pp. 62-66, 2011.

[50] Shaaban, **"Conceptual design of a thermal neutron radiography facility in the cyclotron 30 LC using the MCNPX code,"** *Indian Journal of Pure & Applied Physics (IJPAP)*, Vol. 55, No. 2, pp. 135-144, 2017.

[51] J. Fantidis, **"A study of a transportable thermal neutron radiography unit based on a compact RFI linac,"** *Journal of Radioanalytical and Nuclear Chemistry*, Vol.293, No. 1, pp. 95-101, 2012.

[52] J. Mokhtari, F. Faghihi, & J. Khorsandi, **"Design and optimization of the new LEU MNSR for neutron radiography using thermal column to upgrade thermal flux,"** *Progress in Nuclear Energy*, Vol. 100, pp. 221-232, 2017.

[53] J. S. Hendricks, **"*MCNPX version 2.5. c* (No. LA-UR-03-2202),"** Los Alamos National Laboratory, 2003.

[54] F. Rahmani, and M. Shahriari, **"Hybrid photoneutron source optimization for electron accelerator-based BNCT,"** *Nuclear Instruments and Methods in Physics Research Section A: Accelerators, Spectrometers, Detectors and Associated Equipment*, Vol. 618, No. 1-3, pp. 48-53, 2010.

[55] F. Rahmani, and M. Shahriari, **"Beam shaping assembly optimization of Linac based BNCT and in-phantom depth dose distribution analysis of brain tumors for verification of a beam model,"** *Annals of Nuclear Energy*, Vol. 38, No. 2-3, pp. 404-409, 2011

[56] F., Torabi, S. F., Masoudi, and F. Rahmani, **"Photoneutron production by a 25 MeV electron linac for BNCT application,"** *Annals of Nuclear Energy*, Vol. 54, pp. 192-196, 2013.

[57] S. F. Masoudi, and F. S. Rasouli, **"Investigating a multi-purpose target for electron linac based photoneutron sources for BNCT of deep-seated tumors,"** *Nuclear Instruments and Methods in Physics Research Section B: Beam Interactions with Materials and Atoms*, Vol. 356, pp. 146-153, 2015.

[58] A. Taheri, and A. Pazirandeh, **"Measurements of the thermal neutron flux for an accelerator-based photoneutron source,"** *Australasian physical & engineering sciences in medicine*, Vol. 39, No. 4, pp. 857-862, 2016

[59] M. Tatari, and A. H. Ranjbar, **"Design of a photoneutron source based on 10 MeV electrons of radiotherapy linac,"** *Annals of Nuclear Energy*, Vol. 63, pp. 69-74, 2014.

[60] J. G. Fantidis, **"The use of electron linac for high quality thermal neutron radiography unit,"** *Nuclear Instruments and Methods in Physics Research Section A: Accelerators, Spectrometers, Detectors and Associated Equipment* 908 pp. 361-366, 2018.

[61] D. F. R. Mildner, and G. P. Lamaze, **"Neutron transmission of single-crystal sapphire,"** *Journal of applied crystallography*, Vol. 31, No. 6, pp. 835-840, 1998

[62] Schillinger, **"Estimation and measurement of L/D on a cold and thermal neutron guide,"** *Nondestructive Testing and Evaluation*, Vol. 16, No. 2-6, pp. 141-150, 2001

[63] J. C. Domanus, **"Collimators for thermal neutron radiography: An overview,"** *Markgraf J.F.W. (Ed.)*, 1987

[64] J. C. Domanus, and R. S. Matifield, **"Neutron Radiography Handbook,"** *D. Reidel Publ. Co., Dordrecht*, 1981

[65] G. M. MacGillivray, **"Imaging with neutrons: the other penetrating radiation. In Penetrating Radiation Systems and Applications II,** *International Society for Optics and Photonics*, Vol. 4142, pp. 48-58, December 2000.

[66] M. R. Hawkesworth, **"Neutron radiography. Equipment and methods,"** *Atomic Energy Review*, Vol. 15, No. 2, pp. 169-220, 1977.